Ionic multilayers at the free surface of an ionic liquid, trioctylmethylammonium bis(nonafluorobutanesulfonyl)amide, probed by x-ray reflectivity measurements

Naoya Nishi,[1] Yukinori Yasui,[1] Tomoya Uruga,[2] Hajime Tanida,[2] Tasuku Yamada,[3] Shun-ichi Nakayama,[3] Hideki Matsuoka,[3] and Takashi Kakiuchi[1,a)]

[1]*Department of Energy and Hydrocarbon Chemistry, Graduate School of Engineering, Kyoto University, Kyoto 615-8510, Japan*

[2]*Japan Synchrotron Radiation Research Institute, 1-1-1 Kouto, Sayo, Hyogo 679-5198, Japan*

[3]*Department of Polymer Chemistry, Graduate School of Engineering, Kyoto University, Kyoto 615-8510, Japan*

(Received 26 January 2010; accepted 29 March 2010; published online 30 April 2010)

The presence of ionic multilayers at the free surface of an ionic liquid, trioctylmethylammonium bis(nonafluorobutanesulfonyl)amide ($[TOMA^+][C_4C_4N^-]$), extending into the bulk from the surface to the depth of ~60 Å has been probed by x-ray reflectivity measurements. The reflectivity versus momentum transfer (Q) plot shows a broad peak at $Q \sim 0.4$ Å^{-1}, implying the presence of ionic layers at the $[TOMA^+][C_4C_4N^-]$ surface. The analysis using model fittings revealed that at least four layers are formed with the interlayer distance of 16 Å. $TOMA^+$ and $C_4C_4N^-$ are suggested not to be segregated as alternating cationic and anionic layers at the $[TOMA^+][C_4C_4N^-]$ surface. It is likely that the detection of the ionic multilayers with x-ray reflectivity has been realized by virtue of the greater size of $TOMA^+$ and $C_4C_4N^-$ and the high critical temperature of $[TOMA^+][C_4C_4N^-]$. © *2010 American Institute of Physics*. [doi:10.1063/1.3398029]

I. INTRODUCTION

Ionic liquids (ILs) have attractive properties such as negligibly low vapor pressure, wide liquid ranges, reasonable ionic conductivity, and wide electrochemical window, which can lead to a vast range of applications.[1–4] In many of those applications, the surface and interface of ILs are expected to play crucial roles. Anticipating unique structures and properties at the interfaces of ILs, extensive studies have been conducted in the past decade, using several surface-selective spectroscopic techniques,[5–17] neutron reflectivity (NR)[18] and x-ray reflectivity (XR)[11,19–21] measurements, scanning probe microscopy,[22,23] interfacial tension measurements,[24–35] and molecular dynamics (MD) simulations.[36–41] One of the intriguing features of the IL interfaces is the ion layers, which has been observed at the free surface of ILs by NR[18] and XR[11,19] and at the interface between ILs and a charged sapphire by XR.[20,21] For the latter interface, the ion layers induced by the arrayed charges on the sapphire surface extend into bulk with a depth of several layers.[20,21] The presence of such ionic multilayers has been proposed at the electrochemical interface of molten salts in 1960s,[42,43] and of ILs recently.[44,45] Such multilayer structures at the interface would show intriguing dynamics when it experiences perturbation. We recently found that interfacial tension at the interface between water and an IL, trioctylmethylammonium bis(nonafluorobutanesulfonyl)amide ($[TOMA^+][C_4C_4N^-]$, Scheme 1), exhibits a very slow relaxation when the electric potential difference across the interface is changed.[35] The time constant of the relaxation process is of the order of minutes and is not simply proportional to the viscosity of ILs.[46] This ultraslow relaxation suggests that the structure of the IL in the vicinity of the interface is highly ordered, possibly forming ionic multilayers composed of bulky $TOMA^+$ and $C_4C_4N^-$ ions. Although several MD simulations predicted ionic multilayers at not only IL|solid but also IL|water and IL|air interfaces,[36–38,41] it is still unclear whether the ionic multilayers are formed at such fluid interfaces. In this paper, we report clear evidence of the presence of the ionic multilayers at the free surface of $[TOMA^+][C_4C_4N^-]$.

II. EXPERIMENTAL

A. Preparation of ionic liquid

$[TOMA^+][C_4C_4N^-]$ was prepared from trioctylmethylammonium chloride (Tokyo Chemical Industry) and hydrogen bis(nonafluorobutanesulfonyl)amide (Wako Pure Chemical Industries) by the method described elsewhere.[47] The prepared $[TOMA^+][C_4C_4N^-]$ was then purified by charcoal/silica-gel column chromatography, according to the method presented by Earle *et al.*,[48] which effectively remove trace

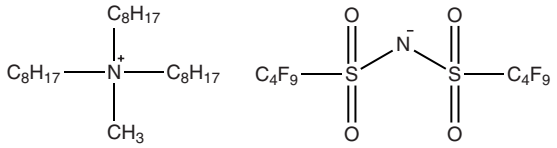

$TOMA^+$ $C_4C_4N^-$

SCHEME 1. Structure of $[TOMA^+][C_4C_4N^-]$.

a)Electronic mail: kakiuchi@scl.kyoto-u.ac.jp.

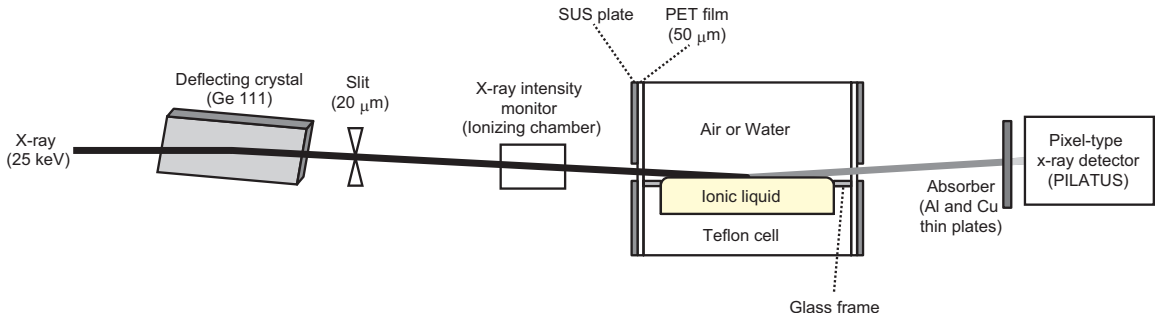

FIG. 1. Scheme of the experimental apparatus for the x-ray reflectivity measurements.

impurities that hamper spectroscopic measurements.[48,49] Impurities were not detected in ^{1}H nuclear magnetic resonance (NMR) and ^{19}F NMR spectra and x-ray fluorescence spectrum measured by a 400 MHz NMR spectrometer (EX-400, Jeol) and x-ray fluorescence analyzer (XGT-1000WR, Horiba), respectively.

B. X-ray reflectivity measurement

XR measurements were performed at the beamline 37XU[50] of SPring-8 using the liquid interface reflectometer[51,52] (Fig. 1). Brilliant undulator x-ray beam with a photon energy of 25 keV (wavelength, λ, of 0.50 Å) was irradiated to the $[TOMA^+][C_4C_4N^-]$ surface. The vertical width of the beam was set to be 20 μm with a slit. We made a PTFE trough that can be used for the IL surfaces (IL|air interface) and also IL|water interfaces (Fig. 1). The lower part of the inside of the trough was filled with IL and the upper part was either air or water. 40 ml of $[TOMA^+][C_4C_4N^-]$ was put into the lower part of the PTFE trough, which has an inner size of $60\times40\times16$ mm^3 (width/depth/height, x-ray is in the direction of the long axis). The incident beam and the beam reflected at the $[TOMA^+][C_4C_4N^-]$ surface passed through two windows made on the wall of the upper part of the PTFE trough which were covered by 50 μm-thickness PET film (G2-50, Teijin DuPont Films). A flat surface is desirable for XR measurements where x ray is irradiated to the surface at grazing angles. Since $[TOMA^+][C_4C_4N^-]$ is composed of hydrophobic ions, $[TOMA^+][C_4C_4N^-]$ wets the PTFE surface. The wetting prevented us to make a flat surface of $[TOMA^+][C_4C_4N^-]$ in the PTFE trough. To avoid this problem, a glass frame was put inside the PTFE trough (Fig. 1). The surface of the glass frame was made hydrophilic by soaking it in KOH-saturated ethanol overnight and washed with plenty of water before measurements. This combination of the PTFE trough and the glass frame enabled us to make a flat surface of $[TOMA^+][C_4C_4N^-]$, and also a flat interface between $[TOMA^+][C_4C_4N^-]$ and water. The incident angle, α, was changed from 0.02° to 0.995°, which corresponds to the values of momentum transfer, Q $(=(4\pi/\lambda)\sin\alpha)$, from 0.01 to 0.44 Å.

The reflected x-ray beam was detected with a two-dimensional hybrid pixel array detector, PILATUS,[53] covering an area of 487×195 pixels with 172 μm/pixel. The reflectivity was evaluated by integrating the peak of the specularly reflected beam intensity after separating the peak from background and by normalizing the peak area by the intensity when the incident beam was directly irradiated to PILATUS. The integration area was 5×13 pixels (in the horizontal and vertical directions, respectively), the center of which was at the peak top. The pixel number in the vertical direction for the integration is important when analyzing data because it determines the resolution of the detector.[51,54,55] The full width of the half maximum of the peak was typically a few pixels. We estimated the angular dispersion caused by possible curvature of the surface by using a geometrical method proposed by Yano and Iijima[55] and found that the dispersion is negligibly small (less than 1% of α). Yano and Iijima also demonstrated that this integration procedure enables us to successfully analyze the XR data.[55] The analysis using the other integration area led to the same results as those described below.

The accumulation time was 1 s at $Q<0.24$ Å^{-1} and was 10 s at $Q\geq0.24$ Å^{-1}. Data from quadruple measurements were averaged and the standard deviation was evaluated. All measurements were performed at 300 ± 1 K. $[TOMA^+][C_4C_4N^-]$ is not hygroscopic because of its high hydrophobicity.[47] $[TOMA^+][C_4C_4N^-]$ employed was quasiequilibrated with the ambient humidity. Reflectivity data did not change for 10 h, during which $[TOMA^+][C_4C_4N^-]$ remained at 300 K and the ambient humidity. No beam damage was detected for the surface and the bulk of $[TOMA^+][C_4C_4N^-]$ after the measurements. Least-squares fitting of models to the experimental data was performed using a software, SALS.[56]

III. RESULTS AND DISCUSSION

Figure 2(a) shows the plots of the reflectivity (R) at the $[TOMA^+][C_4C_4N^-]$ surface against Q. Reflectivity data were obtained with the reasonable standard deviation values as low as reflectivity of 10^{-8} at $Q=0.44$ Å^{-1}. Also shown in Fig. 2(a) is the Fresnel reflectivity (R_F, solid curve) calculated with the density of $[TOMA^+][C_4C_4N^-]$, 1.281 g cm^{-3}, measured using a pycnometer and the atomic scattering factors of atoms constituting $[TOMA^+][C_4C_4N^-]$ at 25 keV.[57,58] The Fresnel reflectivity is a hypothetical reflectivity when the surface is ideally flat without surface roughness or any surface structures including surface layering. Generally, surface roughness due to thermal capillary waves and molecular structures leads to smaller R than R_F at large Q.[59] In Fig. 2(a), the R plot deviates from the R_F curve to lower values at large Q, which is attributable to the roughness of the

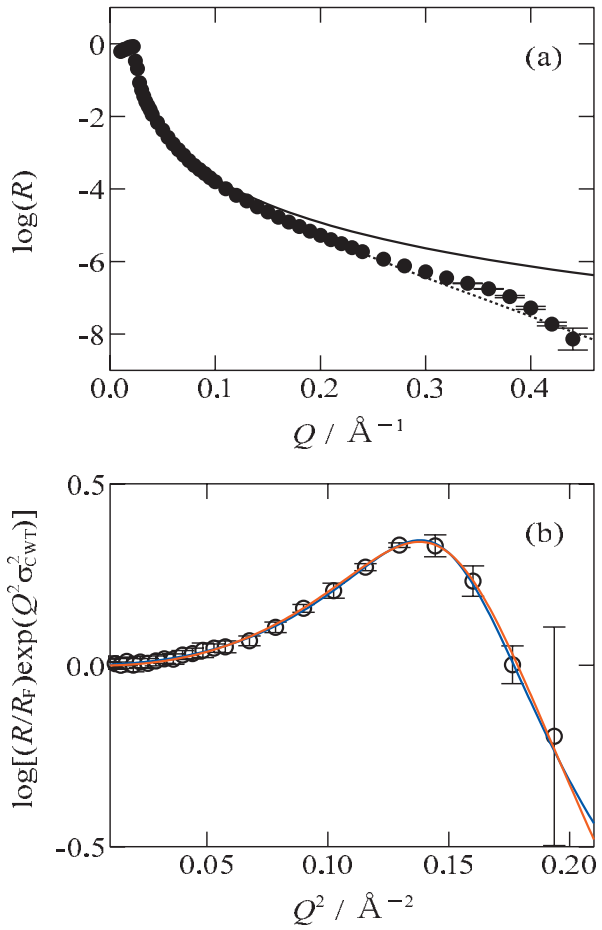

FIG. 2. (a) Plot of x-ray reflectivity (R) vs momentum transfer (Q) with error bars of one standard deviation. The solid curve is the calculated Fresnel reflectivity (R_F) for ideally flat and structureless surface [$\phi=1$ and $\sigma_{CWT}=0$ in Eq. (1)], and the dotted curve is the reflectivity for thermally fluctuated but structureless surface [$\phi=1$ and σ_{CWT} is from Eq. (3)]. (b) $\log[(R/R_F)\exp(\sigma_{CWT}^2Q^2)]$ vs Q^2 plot. The solid curves are from the model fittings for the DC and LC models (red and blue, respectively) to the experimental plots (open circles).

$[TOMA^+][C_4C_4N^-]$ surface. Aside from the deviation from R_F, more importantly, one can see a convex feature around $Q=0.4$ Å^{-1}. A similar convex feature was observed at the free surface of liquids that form surface multilayers,[60–70] indicating the existence of an oscillatory electron density multilayers at the surface of $[TOMA^+][C_4C_4N^-]$ with an interlayer distance of $2\pi/0.4\sim16$ Å. Another hypothetical reflectivity incorporating the surface roughness from the capillary wave theory (see below for the detail) but without any surface structures is also shown in Fig. 2(a) as a dotted curve. One can see that the experimental plots are higher than the dotted curve, which fact suggests that the surface multilayers enhance the reflectivity around $Q=0.4$ Å^{-1}.

For further quantitative analysis of the surface structure of $[TOMA^+][C_4C_4N^-]$, fitting of several models to the reflectivity data was performed. Under the kinematic approximation neglecting multiple scattering, R/R_F as a function of Q can be written as follows:[54]

$$\frac{R}{R_F}=|\phi|^2\exp[-\sigma_{CWT}^2Q^2], \tag{1}$$

TABLE I. Parameters obtained by fitting the curve from the DC model to XR data.

d_{DC} (Å)	$\sigma_{DC,0}$ (Å)	$\bar{\sigma}_{DC}$ (Å)	χ^2 [a]	AIC[b]
15.45 ± 0.10	5.08 ± 0.04	3.35 ± 0.04	4.1	41

[a]Residual error.
[b]AICs for the likelihood of models (Ref. 74). The lower the AIC values of models, the more the likelihood of the models.

$$\phi=\int_{-\infty}^{\infty}\frac{d}{dz}\left(\frac{\langle\rho(z)\rangle}{\rho_\infty}\right)\exp[iQz]dz, \tag{2}$$

where z is a displacement along with the surface normal with $z>0$ for the IL phase, $\langle\rho(z)\rangle$ is an intrinsic electron density averaged in the xy direction (along the surface plane) at z, and ρ_∞ is the electron density in the IL bulk. A surface roughness due to thermal capillary waves derived from the capillary wave theory, σ_{CWT}, may be written as[51,54]

$$\sigma_{CWT}^2=\frac{k_BT}{2\pi\gamma}\ln\left(\frac{q_{max}}{q_{res}}\right), \tag{3}$$

where k_B is the Boltzmann constant, T is the absolute temperature, γ is the surface tension, and q_{max} and q_{res} are the lower and upper cutoffs of the thermal capillary wave vector, respectively. The value of γ for the free surface of $[TOMA^+][C_4C_4N^-]$ was measured in the present study to be 21.9 mN m^{-1} at 300 K using a pendant drop method.[71] The value of q_{max} was estimated to be 0.636 Å^{-1} from $q_{max}=\pi/r$,[54] where r is the radius of the molecule constituting the liquid, and from $r=4.94$ Å, the mean value of radii for $TOMA^+$ and $C_4C_4N^-$ (Table III). The value of q_{res}, which is a function of Q,[54] was evaluated from the sample-detector distance, 1012 mm, and the vertical spatial resolution of PILATUS, 0.172×13 mm^2.[51]

The $\log[(R/R_F)\exp(\sigma_{CWT}^2Q^2)]$ versus the Q^2 plot is shown in Fig. 2(b). The convex feature is prominent in Fig. 2(b) at $Q^2=0.145$ Å^{-2}. We fitted several models of $\langle\rho(z)\rangle/\rho_\infty$ to the experimental data using Eqs. (1)–(3). Box (slab) models up to four boxes did not reproduce the experimental plots (See Fig. S1[72] for the results with three-box and four-box models). On the other hand, the distorted crystal (DC) model[60,61] and the liquid crystal (LC) model,[60,61] both of which incorporate surface multilayers, well reproduced the plots. The fitting results of the DC and LC models are shown as solid lines in Fig. 2(b). In the DC model, the total electron density profile is a superposition of the Gaussian electron density profile in each layer;

$$\frac{\langle\rho(z)\rangle}{\rho_\infty}=\frac{d_{DC}}{\sqrt{2\pi}}\sum_{n=0}^{\infty}\frac{1}{\sigma_{DC,n}}\exp\left[\frac{-(z-nd_{DC})^2}{2\sigma_{DC,n}^2}\right], \tag{4}$$

where d_{DC} is the interlayer distance and $\sigma_{DC,n}$ is the line width for nth layer. The deeper the position of the layer into bulk, the wider the line width; $\sigma_{DC,n}^2=n\bar{\sigma}_{DC}^2+\sigma_{DC,0}^2$, where $\sigma_{DC,0}$ is the line width for the topmost (0th) layer and $\bar{\sigma}_{DC}$ is a factor of the widening of the distribution. In the LC model, surface multilayers are represented as the oscillatory decaying function of the electron density;

TABLE II. Parameters obtained by fitting the curve from the LC model curve to XR data.

d_{LC} (Å)	σ_{LC} (Å)	ξ_{LC} (Å)	z_{LC} (Å)	A_{LC}	χ^2	AIC
16.2 ± 0.4	1.9 ± 0.6	20 ± 2	−2.7 ± 0.8	0.22 ± 0.06	2.08	28.3

$$\frac{\langle\rho(z)\rangle}{\rho_\infty} = \frac{1+\mathrm{erf}\left[\frac{z-z_{LC}}{\sqrt{2}\sigma_{LC}}\right]}{2} + A_{LC}\Theta(z)\sin\left[\frac{2\pi z}{d_{LC}}\right]\exp\left[\frac{-z}{\xi_{LC}}\right], \quad (5)$$

where $\Theta(z)$, A_{LC}, d_{LC}, ξ_{LC}, σ_{LC}, and z_{LC} are the Heaviside function, the amplitude of the oscillation, the period of the oscillation, the factor for the decay, the roughness and its location of the topmost layer due to the structure of ions, respectively, and $\mathrm{erf}(z)=(2/\sqrt{\pi})\int_0^z e^{-t^2}dt$.

As shown in Fig. 2(b) the curves from the DC and LC models well reproduced the experimental data. The parameters obtained by fitting are listed in Tables I and II for the DC and LC models, respectively. The intrinsic electron density profiles using the parameters are shown as solid curves in Fig. 3. For both models, the oscillation of the electron density is discernible up to at least four layers. The distance between layers was evaluated to be ~16 Å from d_{DC} =15.45 Å and d_{LC}=16.2 Å. This value is about 50% greater than ionic diameters for $TOMA^+$ and $C_4C_4N^-$, 10.48 and 9.46 Å, respectively, which are estimated by calculating molar volume of the ion, V_i, by GAUSSIAN 03[73] and by assuming spherical structure ($V_i=(4\pi/3)r_i^3$). Since the actual shapes of $TOMA^+$ and $C_4C_4N^-$ are nonspherical, the 50% greater d is probably due to the alignment of ions with their longer axis preferentially along the surface normal [Fig. 4(a)]. We also used the modified DC (MDC) model[66,69] where the electron density, the line width, and the location of the topmost layer can be different from those in the DC model (see supporting information),[72] but found negligible difference between the obtained electron density profiles from the DC and MDC models (Fig. S2).[72] We used Akaike's information criterion (AIC),[74] a measure of likelihood of models, to find the best model among the DC, LC, and MDC models. We concluded that the LC and MDC models are the most adequate models for the present data (Table SI),[72] although the electron density profile of the MDC model is almost the same as that of the DC model (Fig. S2).[72]

In the DC model, each layer has the same electron density when integrated [see Eq. (4)], which means no segregation of cations and anions between layers as shown in Fig. 4(a). Another possible model for the electron density at the $[TOMA^+][C_4C_4N^-]$ surface is the alternately charged layer (ACL) model where multilayers are alternately composed of cationic and anionic layers. The ACL model was proposed by Mezger *et al.*[20,21] who recently found clear ACLs at the IL interface with a charged sapphire using XR measurements. The ACLs they found seem to be induced by negative charges on the sapphire by x-ray irradiation.[20] Possible ionic arrangements using the ACL model are shown in Figs. 4(b) and 4(c) for the present case at the free surface of $[TOMA^+][C_4C_4N^-]$. The curve from the ACL model did not fit well to our data (Fig. S1).[72] Note that d in Figs. 4(b) and 4(c) is not the interlayer distance but twice for the reflectivity peak to appear at $Q=2\pi/d\sim0.4$ Å in Figs. 2(a) and 2(b). That is why in Figs. 4(b) and 4(c) ions are depicted as oriented with their long axis parallel to the surface plane, not to the surface normal. The orientation of the ions like Fig. 4(a) for the ACL model would result in a peak at Q=0.2 Å in Fig. 2(a) which is not the case with the present data.

An interesting question is why the ionic multilayers were clearly discerned at the free surface for $[TOMA^+][C_4C_4N^-]$ and not for other imidazolium-based ILs studied by XR and NR.[11,18,19] First, the ionic size is large in the case of $[TOMA^+][C_4C_4N^-]$. Table III lists the diameters of IL-constituting ions for the ILs whose free surfaces have been studied by XR and NR. One can see that the sizes of $TOMA^+$ and $C_4C_4N^-$ are 1.3–2 times greater than those of the imidazolium cations and the anions. The greater size leads to the

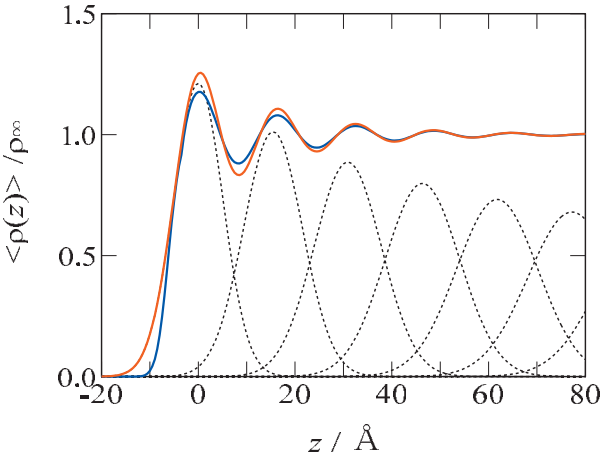

FIG. 3. Intrinsic electron density profiles at the surface of $[TOMA^+][C_4C_4N^-]$ using parameters obtained from the fitting of the DC and LC models (red and blue, respectively) listed in Tables I and II. Gaussian profiles (black dotted lines) correspond to the electron density of ion layers in the DC model. The profile from the LC model is shifted by +3.5 Å to ease the comparison of the two models.

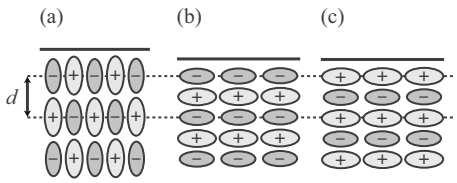

FIG. 4. Simplified schematics of the ionic multilayers at the $[TOMA^+][C_4C_4N^-]$ surface. (a) Ionic layers without segregation of cations and anions between layers, (b) and (c) Ionic layers alternately composed of cations and anions. d is the distance ~16 Å of the repetition depth of the layering structure to show a reflectivity peak at $Q\sim0.4$ $Å^{-1}$.

TABLE III. The ILs used for NR and XR measurements, the diameters of the cations and anions ($2r_c$,$2r_a$) constituting the ILs, and critical temperatures (T_c) of the ILs.

IL	Method	$2r_c$ (Å)	$2r_a$ (Å)	T_c (K)
$[TOMA^+][C_4C_4N^-]$	XR[a]	10.48[b]	9.26[b]	1503.9[c]
$[C_8mim^+]PF_6^-$ [d]	NR[e]	8.28[b]	5.86[b]	810.8,[c] 997,[f] 972[f]
$[C_4mim^+]PF_6^-$ [d]	NR,[e] XR[g,h]	7.16[b]	5.86[b]	719.4,[c] 1240,[f] 1158[f]
$[C_4mim^+]BF_4^-$ [d]	XR[g,h]	7.16[b]	4.95[b]	643.2,[c] 1051,[f] 1007[f]
$[C_4mim^+]I^-$ [d]	XR[h]	7.16[b]	4.4[i]	871.2[c]

[a]The present study.
[b]Estimated from B3LYP/6-311+G** level calculation by GAUSSIAN 03 (Ref. 73).
[c]Evaluated using the spreadsheet provided by Ref. 79.
[d]$C_n mim^+$ is 1-alkyl-3-methylimidazolium, where n is the alkyl chain length.
[e]Reference 18.
[f]Reference 80.
[g]Reference 19.
[h]Reference 11.
[i]Reference 81.

greater interlayer distance, and therefore it is possible to see a reflectivity peak attributable to ionic multilayers at the smaller values of Q. Second, the critical temperature, T_c, of $[TOMA^+][C_4C_4N^-]$ is likely to be high. According to Monte Carlo simulation studies by Chacón *et al.*,[75–78] all kinds of liquids have a possibility to show multilayers at their free surface when the temperature is below $\sim 0.2T_c$. Although most of molecular liquids freeze at such a low temperature, Mo *et al.*[69,70] showed that a molecular liquid, TEHOS, exhibits no evidence of freezing down to 190 K (corresponds to $0.2T_c$). They observed a multilayer by XR below 230 K, $0.23T_c$.[70] The determination of T_c for ILs is difficult because they have negligible vapor pressure and most of them decompose at high temperatures below T_c. The T_c values estimated from the temperature dependence of the surface tension of ILs by Rebelo *et al.*[81] and from the group contribution method by Valderrama and Robles[79,82] are listed in Table III. The imidazolium-based ILs studied by XR and NR are likely to have T_c around 1000 K. Chacón's criteria, $\sim 0.2T_c$, is around 200 K, which is much lower than the temperature for XR and NR measurements so far conducted.[11,18,19] On the other hand, the T_c value for $[TOMA^+][C_4C_4N^-]$ from the group contribution method[79] is estimated to be higher, ca. 1500 K (Table III). The temperature in the present measurements was 300 K, corresponding to $0.2T_c$, around the border of Chacón's criteria[75–77] and lower than $0.23T_c$ for TEHOS.[69,70] Since the melting point of $[TOMA^+][C_4C_4N^-]$ is 272 K,[47] XR measurements at temperatures lower than 300 K would show more pronounced ionic multilayers at the free surface of $[TOMA^+][C_4C_4N^-]$.

In our previous report of the ultraslow response of the interfacial tension at the $[TOMA^+][C_4C_4N^-]$|water interface,[35] we postulated the presence of the ionic multilayers to explain the observation that the inversion of the excess surface charge density by stepping the potential difference across the interface over the potential of zero charge gave rise to a transient increase in the interfacial tension by the transient neutralization of the excess surface charge. The ionic multilayers observed in the present study corroborate the previous postulation, as the rearrangement of the charge ordering over 60 Å from the surface, if exists also at $[TOMA^+][C_4C_4N^-]$|water interface, should require substantial time for reaching a new equilibrium arrangements of $TOMA^+$ and $C_4C_4N^-$ having long alkyl and perfluoroalkyl chains.

IV. CONCLUSIONS

Clear evidence of the ionic multilayers extending into the bulk from the surface with a depth of ~60 Å was obtained at the free surface of $[TOMA^+][C_4C_4N^-]$, which is composed of bulky ions, probably having a high critical temperature. It is interesting to see if this kind of ionic multilayer at the free IL surface exists at other IL interfaces, such as IL|water, IL|organic solvent, and IL|electrode interfaces. From an electrochemical point of view, the response of the ionic multilayer structure against the modulation of the potential drop across the interface is very intriguing and is presumably relevant to a variety of electrochemical applications of ILs.

ACKNOWLEDGMENTS

The authors wish to thank Yohko F. Yano (Ritsumeikan University) for advising us on the data analysis. The authors are also grateful to Yuki Kitazumi and Toshiyuki Motokawa (Department of Energy and Hydrocarbon Chemistry, Graduate School of Engineering, Kyoto University) for their help in the surface tension (YK) and the x-ray reflectivity measurements (TM), respectively. This work has been performed with the approval of SPring-8 (Proposal No. 2008A1200). This work was partly supported by a Grant-in-Aid for Scientific Research (A) (Grant No. 21245021), a Grant-in-Aid for Priority Area (Grant No. 20031017), Grant-in-Aid for Young Research (Grant Nos. 18750062 and 21750075), and the Global COE Program "International Center for Integrated Research and Advanced Education in Materials Science" (Grant No. B-09) from the Ministry of Education, Culture, Sports, Science, and Technology, Japan.

[1] T. Welton, Coord. Chem. Rev. **248**, 2459 (2004).
[2] M. Grätzel, J. Photochem. Photobiol. C **4**, 145 (2003).
[3] M. Galiński, A. Lewandowski, and I. Stępniak, Electrochim. Acta **51**, 5567 (2006).
[4] S. Pandey, Anal. Chim. Acta **556**, 38 (2006).
[5] T. J. Gannon, G. Law, P. R. Watson, A. J. Carmichael, and K. R. Seddon, Langmuir **15**, 8429 (1999).
[6] G. Law, P. R. Watson, A. J. Carmichael, and K. R. Seddon, Phys. Chem. Chem. Phys. **3**, 2879 (2001).
[7] N. Nanbu, Y. Sasaki, and F. Kitamura, Electrochem. Commun. **5**, 383 (2003).
[8] S. Baldelli, J. Phys. Chem. B **107**, 6148 (2003).
[9] T. Iimori, T. Iwahashi, H. Ishii, K. Seki, Y. Ouchi, R. Ozawa, H. Hamaguchi, and D. Kim, Chem. Phys. Lett. **389**, 321 (2004).
[10] J. Sung, Y. Jeon, D. Kim, T. Iwahashi, T. Iimori, K. Seki, and Y. Ouchi, Chem. Phys. Lett. **406**, 495 (2005).
[11] Y. Jeon, J. Sung, W. Bu, D. Vaknin, Y. Ouchi, and D. Kim, J. Phys. Chem. C **112**, 19649 (2008).
[12] C. S. Santos and S. Baldelli, J. Phys. Chem. B **113**, 923 (2009).
[13] N. Nishi, R. Ishimatsu, M. Yamamoto, and T. Kakiuchi, J. Phys. Chem. C **111**, 12461 (2007).
[14] E. F. Smith, I. J. Villar Garcia, D. Briggs, and P. Licence, Chem. Commun. (Cambridge) **2005**, 5633.
[15] C. Kolbeck, T. Cremer, K. R. J. Lovelock, N. Paape, P. S. Schulz, P.

Wasserscheid, F. Maier, and H.-P. Steinrück, J. Phys. Chem. B **113**, 8682 (2009).
[16] A. Ohno, H. Hashimoto, K. Nakajima, M. Suzuki, and K. Kimura, J. Chem. Phys. **130**, 204705 (2009).
[17] K. Nakajima, A. Ohno, M. Suzuki, and K. Kimura, Nucl. Instrum. Methods Phys. Res. B **267**, 605 (2009).
[18] J. Bowers, M. C. Vergara-Gutierrez, and J. R. P. Webster, Langmuir **20**, 309 (2004).
[19] E. Sloutskin, B. M. Ocko, L. Taman, I. Kuzmenko, T. Gog, and M. Deutsch, J. Am. Chem. Soc. **127**, 7796 (2005).
[20] M. Mezger, H. Schröder, H. Reichert, S. Schramm, J. S. Okasinski, S. Schöder, V. Honkimäki, M. Deutsch, B. M. Ocko, J. Ralston, M. Rohwerder, M. Stratmann, and H. Dosch, Science **322**, 424 (2008).
[21] M. Mezger, S. Schramm, H. Schröder, H. Reichert, M. Deutsch, E. J. De Souza, J. S. Okasinski, B. M. Ocko, V. Honkimäki, and H. Dosch, J. Chem. Phys. **131**, 094701 (2009).
[22] F. Endres and S. Z. El Abedin, Phys. Chem. Chem. Phys. **8**, 2101 (2006).
[23] R. Atkin, S. Z. El Abedin, R. Hayes, L. H. S. Gasparotto, N. Borisenko, and F. Endres, J. Phys. Chem. C **113**, 13266 (2009).
[24] G. Law and P. R. Watson, Langmuir **17**, 6138 (2001).
[25] J. G. Huddleston, A. E. Visser, W. M. Reichert, H. D. Willauer, G. A. Broker, and R. D. Rogers, Green Chem. **3**, 156 (2001).
[26] T. Kakiuchi, F. Shigematsu, T. Kasahara, N. Nishi, and M. Yamamoto, Phys. Chem. Chem. Phys. **6**, 4445 (2004).
[27] V. Halka, R. Tsekov, and W. Freyland, Phys. Chem. Chem. Phys. **7**, 2038 (2005).
[28] P. Kilaru, G. A. Baker, and P. Scovazzo, J. Chem. Eng. Data **52**, 2306 (2007).
[29] M. G. Freire, P. J. Carvalho, A. M. Fernandes, I. M. Marrucho, A. J. Queimada, and J. A. P. Coutinho, J. Colloid Interface Sci. **314**, 621 (2007).
[30] R. Ishimatsu, F. Shigematsu, T. Hakuto, N. Nishi, and T. Kakiuchi, Langmuir **23**, 925 (2007).
[31] R. Ishimatsu, N. Nishi, and T. Kakiuchi, Langmuir **23**, 7608 (2007).
[32] M. M. Islam, M. T. Alam, T. Okajima, and T. Ohsaka, J. Phys. Chem. B **111**, 12849 (2007).
[33] R. L. Gardas and J. A. P. Coutinho, Fluid Phase Equilib. **265**, 57 (2008).
[34] M. T. Alam, M. M. Islam, T. Okajima, and T. Ohsaka, J. Phys. Chem. C **113**, 6596 (2009).
[35] Y. Yasui, Y. Kitazumi, R. Ishimatsu, N. Nishi, and T. Kakiuchi, J. Phys. Chem. B **113**, 3273 (2009).
[36] R. M. Lynden-Bell, Mol. Phys. **101**, 2625 (2003).
[37] T. Y. Yan, S. Li, W. Jiang, X. P. Gao, B. Xiang, and G. A. Voth, J. Phys. Chem. B **110**, 1800 (2006).
[38] B. L. Bhargava and S. Balasubramanian, J. Am. Chem. Soc. **128**, 10073 (2006).
[39] R. M. Lynden-Bell, M. G. Del Pópolo, T. G. A. Youngs, J. Kohanoff, C. G. Hanke, J. B. Harper, and C. C. Pinilla, Acc. Chem. Res. **40**, 1138 (2007).
[40] W. Jiang, Y. T. Wang, T. Y. Yan, and G. A. Voth, J. Phys. Chem. C **112**, 1132 (2008).
[41] T.-M. Chang and L. X. Dang, J. Phys. Chem. A **113**, 2127 (2009).
[42] E. A. Ukshe, N. G. Bukun, D. I. Leikis, and A. N. Frumkin, Electrochim. Acta **9**, 431 (1964).
[43] A. D. Graves and D. Inman, J. Electroanal. Chem. **25**, 357 (1970).
[44] A. A. Kornyshev, J. Phys. Chem. B **111**, 5545 (2007).
[45] M. V. Fedorov and A. A. Kornyshev, Electrochim. Acta **53**, 6835 (2008).
[46] Y. Yasui, M.S. thesis, Department of Energy and Hydrocarbon Chemistry, Graduate School of Engineering, Kyoto University, 2009.
[47] N. Nishi, H. Murakami, Y. Yasui, and T. Kakiuchi, Anal. Sci. **24**, 1315 (2008).
[48] M. J. Earle, C. M. Gordon, N. V. Plechkova, K. R. Seddon, and T. Welton, Anal. Chem. **79**, 758 (2007).
[49] R. Guillaume, N. Nishi, and T. Kakiuchi, J. Phys. Chem. B **113**, 15322 (2009).
[50] Y. Terada, S. Goto, N. Takimoto, K. Takeshita, H. Yamazaki, Y. Shimizu, S. Takahashi, H. Ohashi, Y. Furukawa, T. Matsushita, T. Ohata, Y. Ishizawa, T. Uruga, H. Kitamura, T. Ishikawa, and S. Hayakawa, AIP Conf. Proc. **705**, 376 (2004).
[51] Y. F. Yano, T. Uruga, H. Tanida, H. Toyokawa, Y. Terada, M. Takagaki, and H. Yamada, Eur. Phys. J. Spec. Top. **167**, 101 (2009).
[52] Y. F. Yano, T. Uruga, H. Tanida, H. Toyokawa, Y. Terada, M. Takagaki, and H. Yamada, "Characterization of liquid surfaces by advanced x-ray reflection measurements," Bunseki Kagaku (in press).
[53] C. Broennimann, E. F. Eikenberry, B. Henrich, R. Horisberger, G. Huelsen, E. Pohl, B. Schmitt, C. Schulze-Briese, M. Suzuki, T. Tomizaki, H. Toyokawa, and A. Wagner, J. Synchroton Radiat. **13**, 120 (2006).
[54] A. Braslau, P. S. Pershan, G. Swislow, B. M. Ocko, and J. Als-Nielsen, Phys. Rev. A **38**, 2457 (1988).
[55] Y. F. Yano and T. Iijima, J. Chem. Phys. **112**, 9607 (2000).
[56] T. Nakagawa and Y. Oyanagi, in *Recent Developments in Statistical Inference and Data Analysis*, edited by K. Matusita (North-Holland, Amsterdam, 1980), pp. 221–225.
[57] B. L. Henke, E. M. Gullikson, and J. C. Davis, At. Data Nucl. Data Tables **54**, 181 (1993).
[58] See E. Gullikson web page: http://henke.lbl.gov/.
[59] J. Als-Nielsen and D. McMorrow, *Elements of Modern X-Ray Physics* (Wiley, New York, 2001), Chap. 3.
[60] O. M. Magnussen, B. M. Ocko, M. J. Regan, K. Penanen, P. S. Pershan, and M. Deutsch, Phys. Rev. Lett. **74**, 4444 (1995).
[61] M. J. Regan, E. H. Kawamoto, S. Lee, P. S. Pershan, N. Maskil, M. Deutsch, O. M. Magnussen, B. M. Ocko, and L. E. Berman, Phys. Rev. Lett. **75**, 2498 (1995).
[62] M. J. Regan, P. S. Pershan, O. M. Magnussen, B. M. Ocko, M. Deutsch, and L. E. Berman, Phys. Rev. B **55**, 15874 (1997).
[63] H. Tostmann, E. DiMasi, P. S. Pershan, B. M. Ocko, O. G. Shpyrko, and M. Deutsch, Phys. Rev. B **59**, 783 (1999).
[64] O. Shpyrko, P. Huber, A. Grigoriev, P. Pershan, B. Ocko, H. Tostmann, and M. Deutsch, Phys. Rev. B **67**, 115405 (2003).
[65] O. G. Shpyrko, A. Y. Grigoriev, C. Steimer, P. S. Pershan, B. H. Lin, M. Meron, T. Graber, J. Gerbhardt, B. Ocko, and M. Deutsch, Phys. Rev. B **70**, 224206 (2004).
[66] P. S. Pershan, S. E. Stoltz, O. G. Shpyrko, M. Deutsch, V. S. K. Balagurusamy, M. Meron, B. H. Lin, and R. Streitel, Phys. Rev. B **79**, 115417 (2009).
[67] N. Lei, Z. Q. Huang, and S. A. Rice, J. Chem. Phys. **104**, 4802 (1996).
[68] O. G. Shpyrko, R. Streitel, V. S. K. Balagurusamy, A. Y. Grigoriev, M. Deutsch, B. M. Ocko, M. Meron, B. H. Lin, and P. S. Pershan, Science **313**, 77 (2006).
[69] H. D. Mo, G. Evmenenko, S. Kewalramani, K. Kim, S. N. Ehrlich, and P. Dutta, Phys. Rev. Lett. **96**, 096107 (2006).
[70] H. Mo, S. Kewalramani, G. Evmenenko, K. Kim, S. N. Ehrlich, and P. Dutta, Phys. Rev. B **76**, 024206 (2007).
[71] Y. Kitazumi and T. Kakiuchi, Langmuir **25**, 8062 (2009).
[72] See supplementary material at http://dx.doi.org/10.1063/1.3398029 for the other models employed and the fitting results.
[73] M. J. Frisch, G. W. Trucks, H. B. Schlegel, *et al.*, GAUSSIAN 03, Revision D.01, Gaussian, Inc., Pittsburgh PA, 2003.
[74] H. Akaike, IEEE Trans. Autom. Control **19**, 716 (1974).
[75] E. Chacón, M. Reinaldo-Flagán, E. Velasco, and P. Tarazona, Phys. Rev. Lett. **87**, 166101 (2001).
[76] E. Velasco, P. Tarazona, M. Reinaldo-Flagán, and E. Chacón, J. Chem. Phys. **117**, 10777 (2002).
[77] P. Tarazona, E. Chacón, M. Reinaldo-Flagán, and E. Velasco, J. Chem. Phys. **117**, 3941 (2002).
[78] R. Checa, E. Chacón, and P. Tarazona, Phys. Rev. E **70**, 061601 (2004).
[79] J. O. Valderrama and R. E. Rojas, Ind. Eng. Chem. Res. **48**, 6890 (2009).
[80] L. P. N. Rebelo, J. N. Canongia Lopes, J. M. S. S. Esperanca, and E. Filipe, J. Phys. Chem. B **109**, 6040 (2005).
[81] R. D. Shannon and C. T. Prewitt Acta Cryst. **25**, 925 (1969).
[82] J. O. Valderrama and P. A. Robles, Ind. Eng. Chem. Res. **46**, 1338 (2007).